Crystallization kinetics of ZnS precipitation; an experimental study using the mixed-suspension-mixed-product-removal (MSMPR) method

Tarazi, Mousa Al-; Heesink, A. Bert M.; Azzam, Mohammed O.J.; Yahya, Salah Abu; Versteeg, Geert F.

Published in:
Crystal Research and Technology

DOI:
10.1002/crat.200310238

Cryst. Res. Technol. **39**, No. 8, 675 – 685 (2004) / **DOI** 10.1002/crat.200310238

Crystallization kinetics of ZnS precipitation; an experimental study using the mixed-suspension-mixed-product-removal (MSMPR) method

Mousa Al-Tarazi*[1], A. Bert M. Heesink[1], Mohammed O. J. Azzam[2], Salah Abu Yahya[2], and Geert F. Versteeg[1]

[1] Faculty of Science & Technology, University of Twente, Enschede, The Netherlands, www.utwente.nl
[2] Chemical Engineering Department, Jordan University of Science and Technology, Jordan, www.just.edu.jo

Received 22 December 2003, revised 13 February 2004, accepted 1 March 2004
Published online 15 July 2004

Key words precipitation kinetics, nucleation, growth, agglomeration, zinc sulfide.
PACS 81.10.A

The precipitation kinetics of zinc sulfide were studied using a lab scale mixed-suspension-mixed-product-removal (MSMPR) precipitation reactor. The vessel was operated at different feed concentrations, molar ratios, stirrer speeds, pH-values, feed injection positions and residence times. Primary nucleation and volume average crystal growth rates as well as agglomeration kernel were determined. Relationships were found between the rates of the different crystallization steps on the one hand and supersaturation, stirrer speeds, pH-values, Zn^{2+} to S^{2-} ratio, feed positions on the other. These show that larger crystals are obtained at high supersaturation, moderate stirrer speeds, small residence times, a pH-value of around 5 and high Zn^{2+} to S^{2-} ratios. One should realize though that the applied MSMPR method is not the most optimal technique for examining fast precipitation reactions.

1 Introduction

The characteristics of a crystal product with regard to filterability, flowability, drying, caking and tabletting behavior is mainly determined by crystal size distribution, morphology, degree of agglomeration and purity [1]. Many chemical processes, such as the synthesis of catalysts, pigments and pharmaceutical products, offshore oil drilling, and water treatment, involve precipitation in one or more key steps of the overall operation. Precipitation is a very complex process, since it is influenced by several interacting phenomena, and for this reason it has attracted much attention. Precipitation occurs through several steps, namely nucleation, crystal growth, and eventually aggregation and breakup. During the precipitation of sparingly soluble solids, agglomeration competes with molecular ionic crystal growth at the solid-liquid interface [2]. Knowledge of agglomeration behavior is therefore also required.

Reliable kinetic data are of the utmost importance for the successful modeling and scale-up of precipitation processes. Crystallization kinetics (including primary nucleation rates, growth rates and agglomeration kernel) are usually measured using the Mixed-Suspension-Mixed-Products Removal (MSMPR) crystallizer technique [3]. This technique permits the simultaneous determination of nucleation and growth kinetics by measuring particle size distribution (PSD) as a function of average residence time. When precipitating sparingly soluble solids, secondary processes such as agglomeration may also play an important role in determining the product quality. It is quite difficult to distinguish between agglomeration and the crystal growth kinetics [4]. However,

* Corresponding author: e-mail: m.y.m.al-tarazi@ct.utwente.nl

MSMPR experiments can also be used to predict agglomeration kernel. This kernel can be obtained from the population balances in volume coordinates while assuming size independent agglomeration behavior.

Narayan and Patwardhan (1992) studied the agglomeration of copper sulfate pentahydrate, nickel ammonium sulfate, potassium sulfate and soy protein in an MSMPR crystallizer [5]. Alan Jones et al. (1996) developed a model for particle formation during agglomerative crystal precipitation [6]. Zuoliang and Palosaari (1997) developed a model to analyze nucleation and growth in a non-ideal MSMPR crystallizer [7]. Their model takes the effects of mixing intensity and product removal location on the size distribution of the produced particles into account. Leubner (1998) has developed a new crystal nucleation theory for the continuous precipitation of silver halides [8]. Jones and Zauner (2000) studied the precipitation kinetics of calcium oxalate in an MSMPR reactor [9]. They concluded that crystal growth proceeds along a surface-integration controlled mechanism with a second order dependence on absolute supersaturation. Jones et al (2001) developed a model to describe agglomerative crystal precipitation based on the Monte Carlo simulation technique [3]. Al-Tarazi et al (2003) studied the precipitation kinetics of copper sulfide using a lab scale MSMPR precipitation reactor [10]. They found that larger crystals are obtained at high supersaturation, moderate stirrer speeds, small residence times, a pH-value of around 5 and high Cu^{2+} to S^{2-} ratios.

This work comprises an experimental study to determine the crystallization kinetics of zinc sulfide also using a lab-scale MSMPR reactor. The effects of supersaturation, pH, molar ratio, feed positions and stirrer speed on the rates of nucleation, growth and agglomeration kernel are studied.

2 Theory

The processes of nucleation, growth and agglomeration interact in a crystallizer and all contribute to the particle size distribution (PSD) of the products [11]. Kinetic data needed for crystallizer design purposes can be obtained with a laboratory scale mixed-suspension, mixed-product removal (MSMPR) crystallizer.

When using this method, It is assumed that all crystals have the same shape and do not break down due to attrition, that the reactor volume is constant, that there are no crystals in the feed, that steady state operation is established and that crystals do not redissolve. It is further assumed that the particles are so small that the growth rate is independent of particle size [5] and that the residence time of the crystals equals that of the solution. The following equation then describes the population balance:

$$G_v \frac{dn}{dv} + \frac{n}{\tau} = B - D \tag{1}$$

G_v represents the volume average growth rate (m^3/s) and n the crystal population density expressed as a function of crystal volume ($\#/m^3.m^3$). B and D represent the empirical birth and death functions over a volume range of v. Birth and death due to agglomeration of two particles having volumes u and v - u leading to the formation of a particle with volume v, are given by the following functions [5]:

$$B = \frac{1}{2}\int_0^v \beta(u, v-u)n(u,t)n(v-u)du \tag{2}$$

$$D = n(v)\int_0^\infty \beta(u,v)n(u)du \tag{3}$$

The agglomeration kernel $\beta(u, v-u)$ is a measure of the frequency of collisions between particles of volumes u and $v - u$ that yield a particle of volume v. The factor ½ in equation (2) prevents that such collisions are counted twice. The agglomeration kernel can be described assuming it to be size-independent, or assuming Brownian motion, gravitational settling, shear, particle inertia or empirical Thomson's kernel as mechanism

[12]. Depending on the chosen mechanism equations (2) and (3) can be integrated and incorporated in the population balance.

Moment μ_j is defined as follows:

$$\mu_j = \int_0^\infty n(v) \quad v^j dv \qquad j = 0, 1, 2, 3,..,m \tag{4}$$

Assuming the agglomeration kernel to be independent on particle size, the population balance (equation 1) can be rewritten in moments notation using equations (2) and (3):

$$-B_o + \frac{\mu_o}{\tau} = -\frac{1}{2}\beta_o \mu_o^2 \tag{5}$$

$$\frac{\mu_1}{\tau} = G_v \mu_o \tag{6}$$

$$\frac{\mu_2}{\tau} = 2G_v \mu_1 + \beta_o \mu_1^2 \tag{7}$$

The rates of nucleation, crystal growth and agglomeration kernel observed in a series of experiments can be correlated using empirical kinetic relations [5]:

$$G_v = k_g (S-1)^g \tag{8}$$

$$B_o = K_R G_v^i \varphi_T^j \tag{9}$$

$$\beta_o = k_\beta G_v^h B_o^p \tau^q \tag{10}$$

Equations (1 to 10) are used to derive kinetic data from MSMPR experiments. In these experiments reactants A and B are continuously added to the reactor. When steady state operation is established a sample of the effluent is taken for analysis. The sample is then analyzed using e.g. Laser Doppler Diffraction to determine average particle size (L_{50}), average surface area (a_T) and solids hold up (φ_T) as well as particle number density as a function of particle size. On the basis of these measurements the rates of nucleation, growth and agglomeration kernel can be calculated at different values of supersaturation. Making use of equations (1) to (10), a set of (G_v, B_o and β_o)-data is obtained. After plotting the values of G_v, B_o and β_o as a function of supersaturation, one can make use of any fitting software to calculate the values of k_g, g, K_R, i, j, k_β, h, p and q in equations (8), (9) and (10) [5].

In this work the crystallization kinetics of zinc sulfide have been examined using a laboratory scale MSMPR crystallizer.

3 Experimental

In order to investigate precipitation kinetics and to determine the parameters influencing crystallization kinetics, experiments have been carried out using the MSMPR method at different feed concentrations, stirrer speeds, residence times, feed positions and molar ratios.

The experimental setup (see Figure 1) consisted of a gastight reactor out of glass that was equipped with a multi speed disk & blade mixer and four baffles. The reactor had a volume of 750 ml and a diameter of 11 cm and was connected to a pressure indicator and a thermometer. A jacket around the reactor enabled temperature control. Two peristaltic feed pumps and one withdrawing suction pump were used to adjust the flows of the feed streams and the effluent stream respectively. The liquid hold up was kept constant by using an overflow system by which the liquid level could be controlled. The reactor was thermostated by using either cooling or heating water. All experiments were carried out at ambient temperature (i.e. 20°C). The sulfide concentration in the crystallizer as well as the pH were measured online using ion selective electrodes. The feed streams (i.e. solutions of zinc sulfate and sodium sulfide) were introduced into the crystallizer via stainless steel tubes that could be positioned at different locations inside the reactor. Because zinc sulfide exhibits a tendency to agglomerate, small amounts of detergent (Triton X100) were added to the samples to inhibit agglomeration of the crystals (0.1 ml of X-100/1000 ml of sample). The reactor was operated under nitrogen and at a constant overpressure of 0.1 atm to prevent the oxidation of sulfide ions by air/oxygen. Even at high stirring speeds bubble formation could be avoided and the contact between gas and liquid always was minimal to reduce possible oxidation of produced ZnS crystals, the formation of poly-sulfide and H_2S stripping. The particle size distribution of the produced crystals was measured within 10 minutes after sampling.

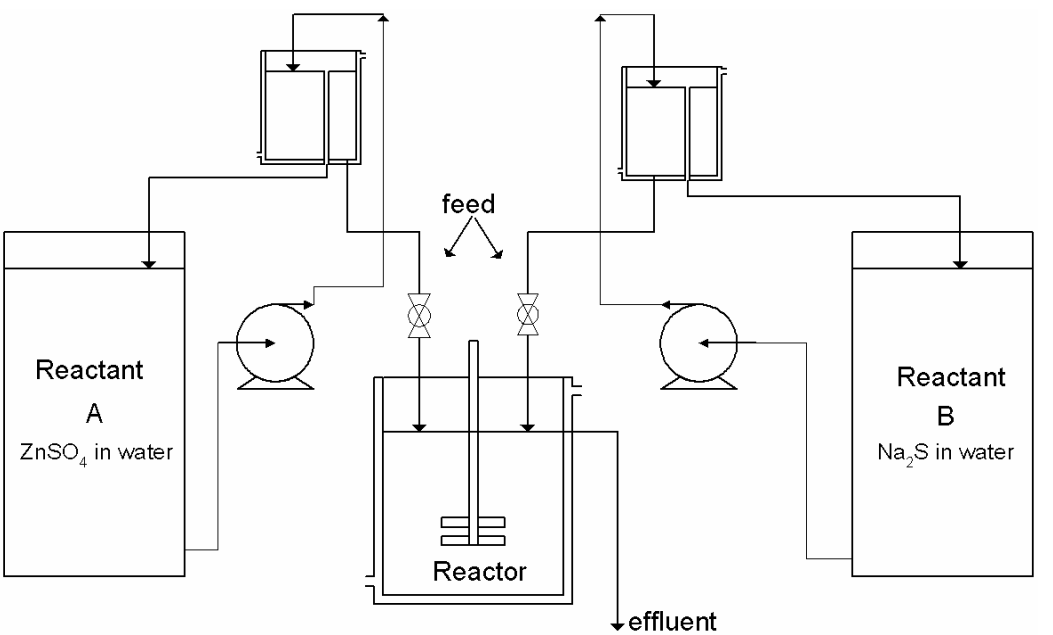

Fig. 1 Applied laboratory scale MSMPR crystallizer.

To ensure that steady state was reached when sampling, the pH was continuously monitored. It was observed that steady state was always achieved after 12-14 average residence times. After that, 500 ml of effluent was collected for analysis. X-ray diffraction (Microtrac X100, size range 0.45 -1000 microns) and a Zeta-sizer (Zetasizer 5000, size range 1-5000 nm) were used to determine particle size distribution. Atomic absorption spectroscopy (AAS) was used to measure the concentration of free zinc ions in the effluent. The sample was filtered, dried and weighed to check the zinc balance. Solids hold up was calculated from the mass balance of the zinc ions. Particle volume density was calculated from the solids hold up and the particle size distribution using the following formula:

$$n_i = \varphi_T \frac{v\%}{\rho_s (v_p)_i ((v_p)_i - (v_p)_{i-1})} \qquad \textit{where i represents the class number} \qquad (11)$$

4 Results and discussion

In order to investigate the crystallization kinetics of zinc sulfide several experiments were conducted at different feed concentrations (supersaturations), stirrer speeds, residence times, feed molar ratios, feeds positions and pH-values. Supersaturation was calculated on basis of the feed concentrations of both zinc and sulphide ions while using equation (12)

$$S = \sqrt{\frac{[Zn^{2+}][S^{2-}]}{K_{sp}}} \tag{12}$$

The effect of relative supersaturation on the volume average growth rate of the produced particles is shown in Figure 2. Relative supersaturation was varied over a wide range (from $1x10^8$ to $5x10^{10}$) while keeping the molar ratio at 1. The volume average growth rate (G_v) was found to vary from $5x10^{-19}$ to $9x10^{-18}$ m^3/s. In general the growth rate of ZnS is higher than that earlier obtained for CuS (G_v = $1x10^{-20}$ to $1.2x10^{-19}$) [10]. A logarithmic fit delivers:

$$G_v = 9.77x10^{-23}(S-1)^{0.47} \tag{13}$$

the growth rate constant (k_g) being $9.77x10^{-23}$ m^3/s for the applied conditions.

The reaction between zinc ions and sulphide ions was found to be very fast, but only at supersaturations higher than $1.9x10^{10}$ complete conversion was achieved whereas at lower supersaturation a conversion of typically 75% was found. The average size of the produced particles was varying from 1 micron at low relative supersaturation ($7.5x10^7$) to 9.1 microns at higher relative supersaturations. The obtained average particle size is expressed as a function of supersaturation by equation (14). The volume average growth rate can be rewritten in terms of linear growth rate yielding equation (15). By substituting equation (14) into equation (15) one may conclude that linear growth proceeds through the mechanism of polynucleation [13].

$$d_s = 1.44x10^{-8}(S\text{-}1)^{0.35} \tag{14}$$

$$G_v = \frac{\pi}{2} d_s^2 G_L \tag{15}$$

$$G_L = 2.98x10^7(S-1)^{-0.3} \tag{16}$$

The linear growth rate (equation 16) apparently decreases with supersaturation. This is probably due to the assumption of independent size growth, which is not necessarily valid.

In order to arrive at a function of the form of equation (9) the observed primary nucleation rate has been expressed as a function of volume average growth rate and solids hold up using a fitting correlation. The Newton method for multi-dimensional optimization was used to calculate the best-fit coefficients for equation (9):

$$B_o = 1.66x10^{-18} G_v^{-1.76} \varphi_T^{1.6} \tag{16}$$

Figure 3 shows the values calculated with this correlation versus the experimentally observed values. An increase of the volume average growth rate corresponds to a decrease in nucleation rate as to be expected. However increasing the solids holdup yields a more than proportional increase in primary nucleation rate which may be related to higher agglomeration rates at higher solids hold up. Substituting the observed effects of supersaturation on volume growth rate [$G_v = 9.77x10^{-23}(S\text{-}1)^{0.47}$] and solids hold up [$\varphi_T = 1.2x10^{-7}\ (S\text{-}1)$] delivers the relationship between supersaturation and primary nucleation rate:

$$B_o = 9.31x10^9(S\text{-}1)^{0.77} \tag{17}$$

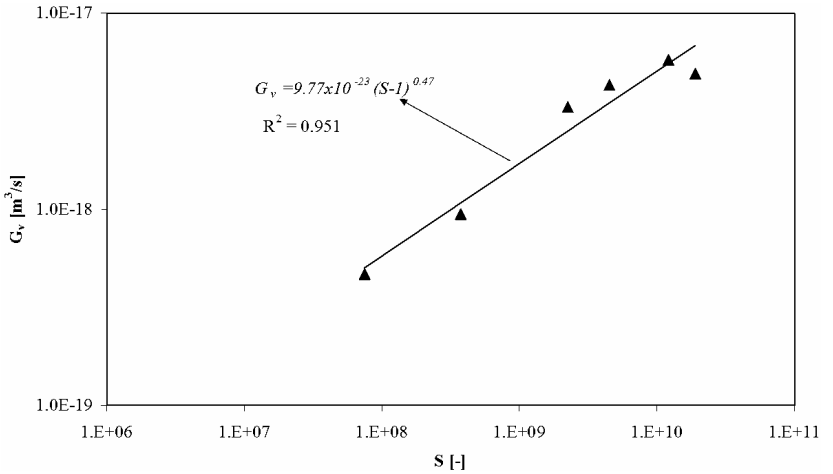

Fig. 2 Logarithmic plot of volume average growth rate vs. relative supersaturation (S): the solid line represents the fitting equation. RPM = 720, molar feed ratio Zn^{2+}:S^{2-} = 1:1, pH=5.6, residence time = 157 s

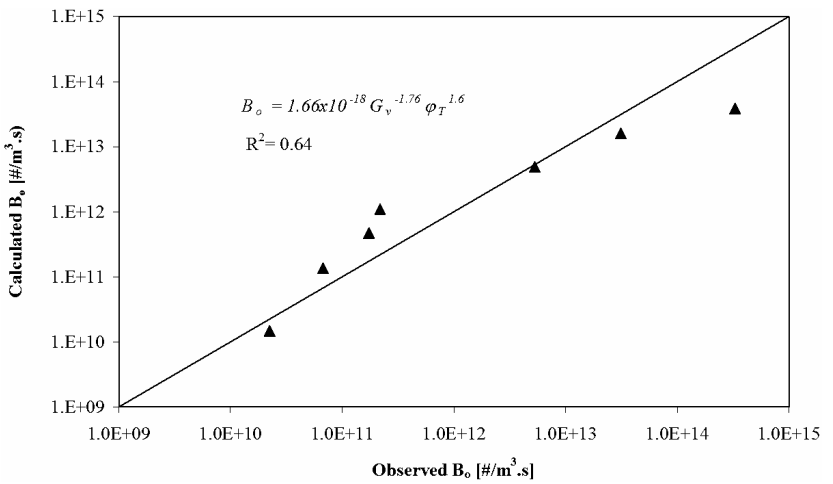

Fig. 3 Calculated rate using the proposed fitting equation vs observed primary nucleation rate; RPM = 720, molar feed ratio Zn^{2+}: S^{2-} = 1:1, pH=5.6, residence time = 157 s, $[Zn^{2+}]_{inlet}$= $[S^{2-}]_{inlet}$ = 8.9 x $10^{-2} \sim 2.8x10^{1}$ mol/m^3.

This relation shows that an increase in supersaturation corresponds with an increase in primary nucleation rate. In theory, the primary nucleation rate is expected to be highly dependent on supersaturation (the exponent in equation (17) is expected to be in between 5 and 15 [11, 13]). This result can be explained by the fact that the rate of agglomeration also increases with supersaturation, thereby suppressing the primary nucleation rate and enhancing the observed average volume growth rate. Agglomerates grow faster than a single small particle and hence primary nucleation becomes less apparent [14].

Agglomeration kernel was calculated from the experimental results using equation (10). The experimental results were fitted by means of nonlinear regression to identify the relationship between agglomeration kernel on the one hand and primary nucleation rate and volume average growth rate on the other (as expressed by equation (10)). See Figure 4. Although the fit is certainly not perfect we can conclude that an increase of the primary nucleation rate and a decrease of the average volume growth rate correspond with an increase in agglomeration kernel as to be expected [13]:

$$\beta_o = 2.27x10^{-44} B_o^{0.3} G_v^{-1.47} \tag{18}$$

As residence time was not varied the factor t^q (in equation 10) has been included in the value of k_β (=2.268x10^{-44} $m^{6.5}/\#^{1.3}.s^{-0.3}$) in equation (18). An increase in the primary nucleation rate increases the agglomeration kernel while an increase in the volume average growth rate decreases the agglomeration kernel.

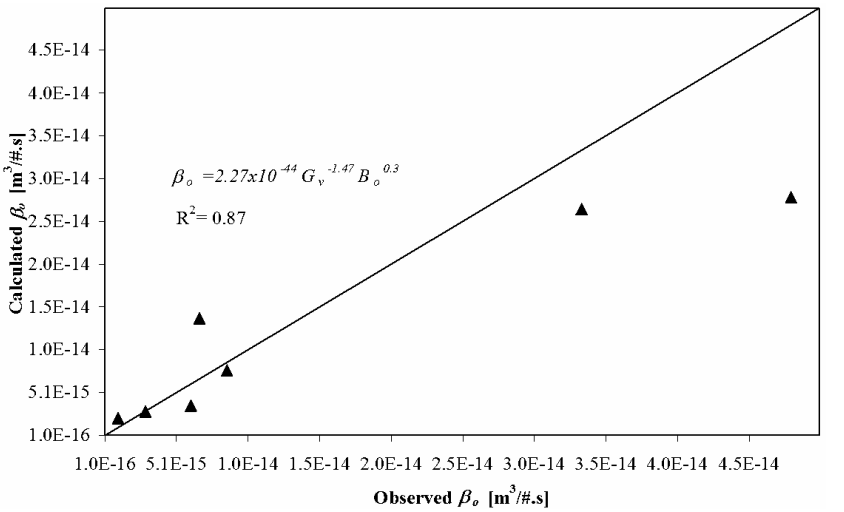

Fig. 4 Calculated agglomeration kernel using the proposed fitting equation vs. observed kernel. RPM = 720, molar feed ratio Zn^{2+}:S^{2-} = 1:1, pH=5.6, residence time = 157 s, $[Zn^{2+}]_{inlet}$= $[S^{2-}]_{inlet}$ = 8.9x10^{-2}~2.8x10^{1} mol/m^3 .

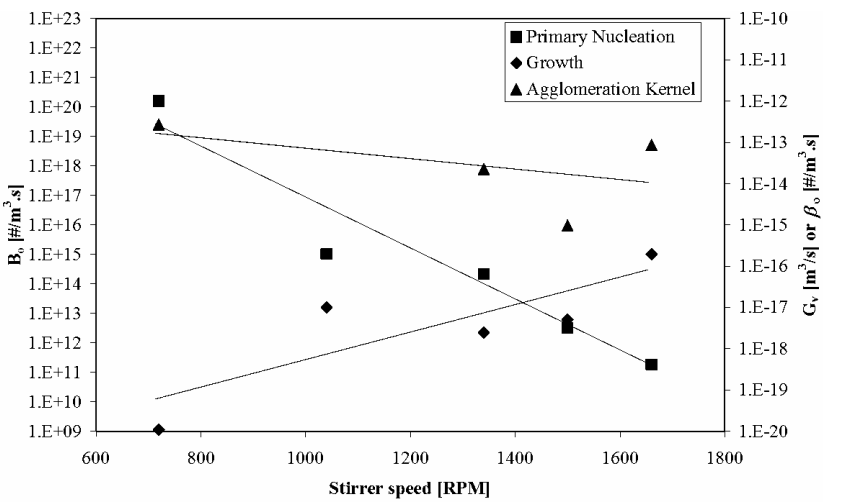

Fig. 5 Effects of stirrer speed on volume average growth rate, primary nucleation rate and agglomeration kernel. Molar feed ratio Zn^{2+}:S^{2-} = 1:1, pH=5.6, residence time = 157 s, $[Zn^{2+}]_{inlet}$ = $[S^{2-}]_{inlet}$=8.9 mol/m^3 .

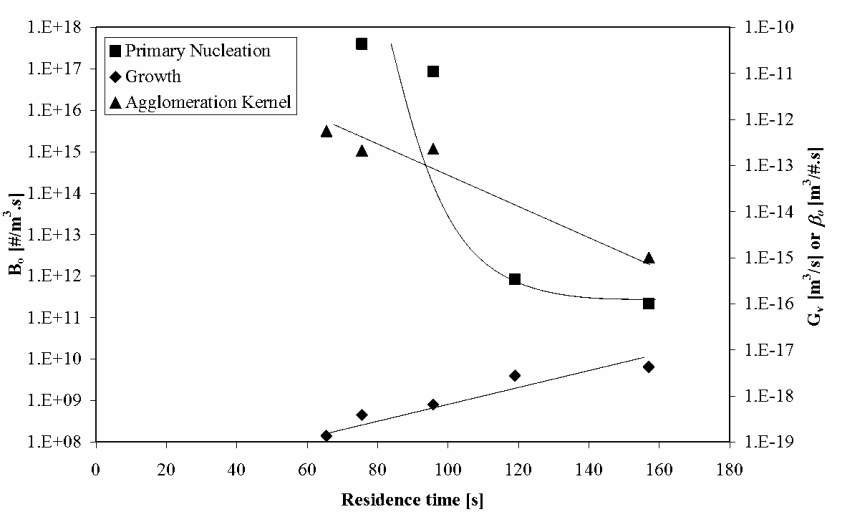

Fig. 6 Effects of residence time on volume average growth rate, primary nucleation rate and agglomeration kernel. Molar feed ratio Zn^{2+}:S^{2-} = 1:1, RPM = 720, pH=5.6, $[Zn^{2+}]_{inlet}$=$[S^{2-}]_{inlet}$= 8.9 mol/m^3 .

In general, increasing supersaturation corresponds with a decrease in agglomeration kernel (β_o=5.6x10^{-9}(S-1)$^{-0.5}$). Collisions of bigger particles (occurring at higher G_v- values) are more successful in producing agglomerates. Also an increase in particle concentration will raise agglomeration kernel due to an increase in collision frequency.

The effects of stirrer speed on the volume average growth rate of the ZnS crystals, primary nucleation rate and agglomeration kernel are demonstrated in Figure 5. As can be seen increasing the stirrer speed increases the observed growth rate. Increasing the stirrer speed results in a decrease in local supersaturation near the feed points, which would indeed make the conditions more favorable for crystal growth than for primary nucleation. By increasing the stirrer speed the collision frequency will increase leading to more agglomerates. A further increase of the stirrer speed is expected to cause more disruption of the agglomerated particles resulting in a reduction in particle size and G_v. However, we did not observe this in the range of the stirred speeds applied in this work. As the rate of volume average crystal growth is increasing while the primary nucleation rate is decreasing, agglomeration kernel will lower as stirrer speed is increased. A decrease in the number of particles will decrease the collision frequency resulting in lower β_o-values.

Figure 6 shows the effects of residence time on volume average growth rate, primary nucleation rate and agglomeration kernel. Residence time was changed by adjusting the feed flowrates while keeping all other conditions constant. An increase in residence time results in an exponential increase in volume average growth rate. The primary nucleation rate and the agglomeration kernel were found to decrease with residence time. Increasing the residence time by decreasing the feed flowrate (while keeping the stirrer speed constant) will lead to lower local supersaturation values at the feed points. As the rate of crystal growth is less dependent on supersaturation than that of primary nucleation, new formed ZnS-molecules will increasingly tend to attach to existing crystals instead of forming new nuclei as residence time is increased. This results in a drop in number of particles. On the other hand increasing the residence time of the particles inside the reactor will raise the number of particle collisions resulting in more agglomeration. The net effect, however appears to be negative as the agglomeration kernel decreases with increasing residence time in the reactor.

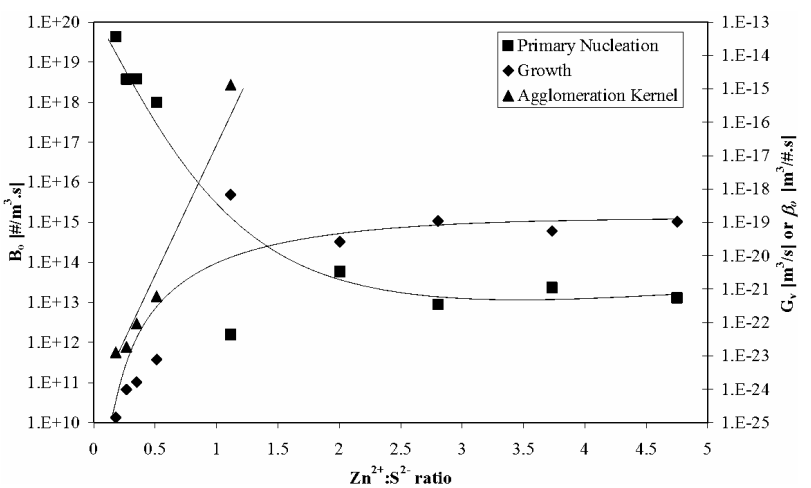

Fig. 7 Effects of molar feed ratio on the volume average growth rate, primary nucleation rate and agglomeration kernel. Conditions: RPM = 720, pH=5.6, residence time = 157 s, $[Zn^{2+}]_{inlet}$ =2.6~14.3 mol/m^3, $[S^{2-}]_{inlet}$ = 3 ~ 15 mol/m^3 .

Figure 7 shows the effects of molar feed ratio (Zn^{2+}:S^{2-}) on the volume average growth rate, primary nucleation rate and agglomeration kernel respectively. The ratio has been adjusted by changing the feed concentrations of Zn^{2+} or S^{2-} while keeping all other parameters constant. Zinc conversion was around 56% when the Zn^{2+} to S^{2-} ratio was higher than unity (instead of typically 75% at a ratio of 1). Increasing the Zn^{2+} to S^{2-} ratio was found to increase the volume average growth rate and agglomeration kernel while decreasing the primary nucleation rate. No large effects were found at Zn^{2+} to S^{2-} ratios higher than 2. This can be explained by the fact that at small Zn^{2+} to S^{2-} ratios (realized by increasing the S^{2-} concentration) polysulfides were observed. These consume the sulfide ions and hence decrease enhance crystal growth.

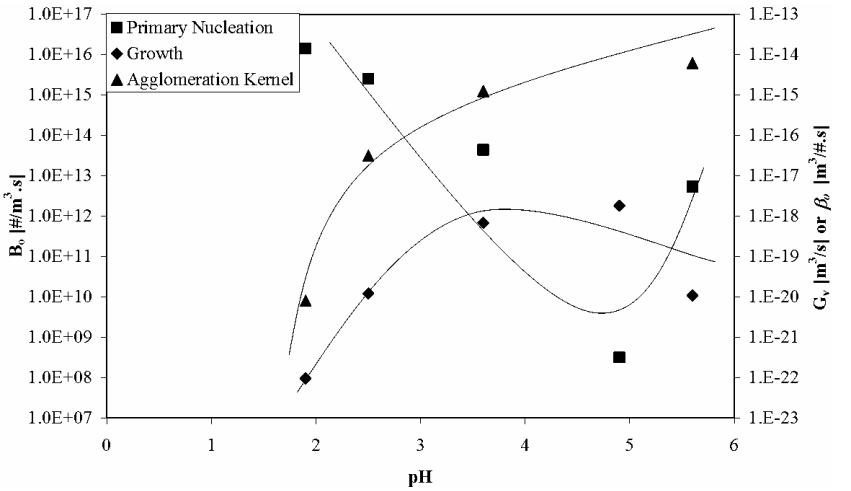

Fig. 8 Effects of pH on volume average growth rate, primary nucleation rate and agglomeration kernel. Conditions: molar feed ratio Zn^{2+}:S^{2-} = 1:1, RPM = 720, $[Zn^{2+}]_{inlet}$ = $[S^{2-}]_{inlet}$ = 8.9 mol/m^3, residence time 157 s.

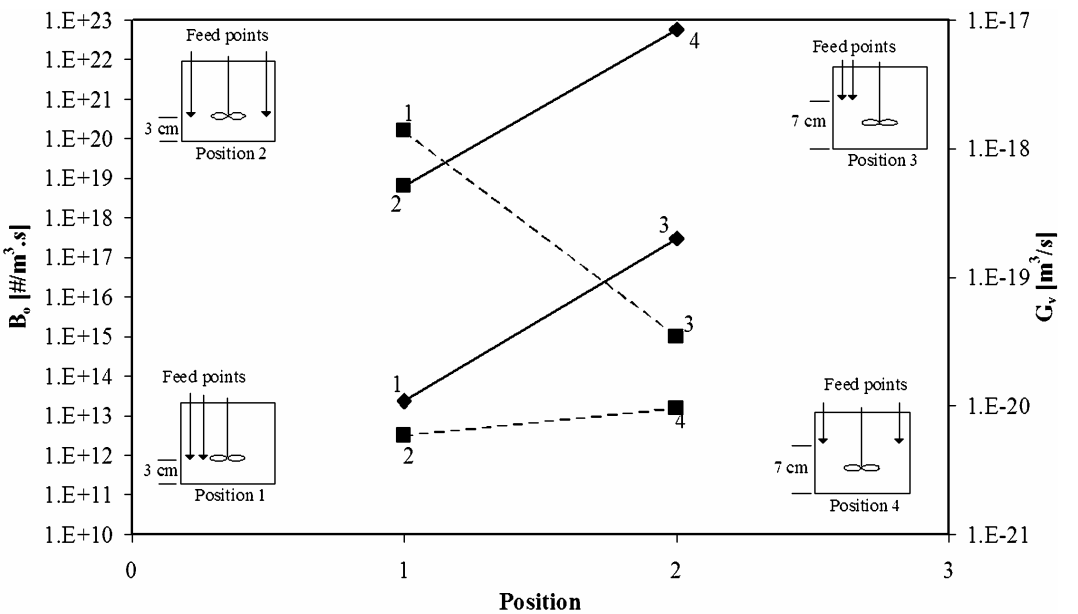

Fig. 9 Effects of feeds positions on volume average growth (♦) and primary nucleation rates (■). Conditions: molar feed ratio Zn^{2+}:S^{2-} = 1:1, RPM = 720, $[Zn^{2+}]_{inlet}$=$[S^{2-}]_{inlet}$=8.9 mol/m^3,residence time 157 s, pH = 5.6.

Figure 8 shows the effects of pH on volume average growth rate, primary nucleation rate and agglomeration kernel respectively. The pH was adjusted by adding sulfuric acid to the Zn^{2+} feed stream. In all experiments 50~90% conversion of Zn^{2+} was observed. Increasing the pH up to a value of about 5 increases the volume average growth rate and agglomeration kernel whereas it decreases the primary nucleation rate. One can thus conclude that a pH-value of around 5 is optimum when large crystals are to be produced. This can be due to the relation between crystal growth and the electrical charge at the crystal surface, which seems to reverse at a pH value of about 5 (the so-called iso-electric point).

Figure 9 shows the effects of injection point positioning on the average volume growth rate and primary nucleation rate. Four cases were tested; see Figure 9. The lowest G_v-value was obtained at position 1 while the highest value was achieved at position 4. On the other hand the primary nucleation rate was found to be highest at position 1 and lowest at position 2. When the injection points are placed adjacent to eachother, local supersaturation is higher which encourages primary nucleation and reduces the volume average growth rate. At

positions 2 and 3 reactants are more diluted before they meet eachother and therefore precipitation occurs at lower supersaturation which is advantageous for crystal growth.

5 Conclusions

The size distribution of particles produced in a crystallizer depends on the kinetics of nucleation and crystal growth. In a precipitation process where solids are formed with an extremely low solubility it is also strongly influenced by agglomeration. This work was concerned with the characterization of crystallization kinetics (primary nucleation, crystal growth and agglomeration) of ZnS using an MSMPR crystallizer (see Table 1). Crystallization kinetics of ZnS were found to depend on supersaturation, stirrer speed, pH, molar feed ratio and residence time. An increase in supersaturation leads to an increase in volume average crystal growth rate, agglomeration kernel and primary nucleation rate. However, one should bear in mind that these results were influenced by unknown mixing phenomena as has been demonstrated by varying stirrer speed and feed injection point positioning. Using the obtained kinetic data for design or scale up purposes can therefore be dangerous. In a future paper we will present an alternative method to measure intrinsic crystallization kinetics in the absence of unknown hydrodynamic phenomena. The results could be used though for similar reactor types than the one applied in this work.

Table 1 ZnS crystallization kinetic.

Growth	$G_v = 9.77x10^{-23}(S-1)^{0.47}$
Primary nucleation	$B_o = 1.66x10^{-18} G_v^{-1.76} \varphi_T^{1.6}$
Agglomeration kernel	$\beta_o = 2.27x10^{-44} B_o^{0.3} G_v^{-1.47}$

Acknowledgments This project was supported with a grant of the Dutch Program EET (Economy, Ecology, Technology) a joint initiative of the Ministries of Economic Affairs, Education, Culture and Sciences, and of Housing, Spatial Planning and Environment. This program is coordinated by the EET Program Office, a partnership of Senter and Novem.

List of symbols

a_T	Specific surface area of the produced particles [m^2/m^3]
B	Secondary nucleation rate [$\#/m^3.m^3.s$]
B_o	Primary nucleation rate [$\#/m^3.s$]
D	Death rate [$\#/m^3.m^3.s$]
d_s	Sauter average particle size [m]
g	Supersaturation exponent in the growth rate correlation [-]
G_L	Linear average crystal growth rate [m/s]
G_v	Volume average crystal growth rate [m^3/s]
h	Exponent of growth rate in the agglomeration kernel correlation [-]
i	Exponent of growth rate in the primary nucleation correlation [-]
j	Exponent of solid holdup in the primary nucleation correlation [-]
k_β	Rate coefficient for agglomeration kernel [$m^3/\#.s$]
k_g	Growth rate constant [m/s]
K_R	Relative nucleation rate constant [$\#/m^3.s$]
K_{sp}	Solubility constant [mol^2/m^6]
n	Crystal volume population density [$\#/m^3.m^3$]
p	Exponent of nucleation rate in agglomeration correlation [-]
q	Exponent of mean residence time in agglomeration correlation [-]
S	Relative supersaturation [-]

t	Time [s]
V	Volume of reactor [m^3]
v	Volume [m^3]
v_p	Volume of particle [m^3]
$\dot{V}$	Volumetric flowrate [m^3/s]
σ	Absolute relative supersaturation [-]
φ_T	Solid holdup [kg/m^3]
β	Agglomeration kernel in volume coordinates [$m^3/\#.s$]
β_o	Size independent agglomeration kernel in volume coordinate [$m^3/\#.s$]
μ_j	Moment of j
τ	Residence time [s]
ρ_s	Density of solids [mol/m^3]
ν	Sctoichiometric ratio [-]
#	Number [-]

References

[1] Herman J. M. Kramer, Sean K. Bermingham, and Gerda M. van Rosmalen. J. Cryst. Growth **198/199**, 729–737 (1999).
[2] A. G. Jones, J. Hostomsky, and Shun Wachi, Chem. Eng. Comm. **146**, 105–130 (1996).
[3] A. G. Jones, G. O. Falope, and R. Zauner, Chem. Eng. Sci. **56**, 2567–2574 (2001).
[4] H. Hatakka, P. Oinas, J. Reunanen, and S. Palosaari, Chem. Eng. Comm. **146**, 76–78 (1996).
[5] Narayan S. Tavare and Anand V. Patwardhan, AIChE J. **38**, 3 (1992).
[6] Alan G. Jones, Jiri Hostomsky, and Shun Wachi, Chem. Eng. Comm. **146**, 105–130, (1996).
[7] Zuoliang Sha and Seppo Palosaari, Scand. Chem Technol. Ser. **244**, 79–81 (1997).
[8] Ingo H. Leubner, J. Imaging Sci & Tec. **42**, 4 (1998).
[9] Alan G. Jones and Rudolf Zauner, Chem. Eng. Sci. **55**, 4219–4232 (2000).
[10] Al-Tarazi Mousa, A. Bert M. Heesink, Mohammed O. J. Azzam, Salah Abu Yahya, and Geert F. Versteeg, Submitted to Journal Separation Science, (2004).
[11] J. W. Mullin, Crystallization, third edition, plant tree, London-UK, (1992).
[12] A. S. Bramley, M. J. Hounslow, and R. L. Ryall, J. Coll. Sci. **183**, 155–165 (1996).
[13] A. Mersmann, Crystallization technology handbook, New York (1995).
[14] M. J. Hounslow, A. S. Bramley, R. Newman, W. R. Paterson, and C. Pogessi, Trans IchemE **75**, 119–124 (1997).